[1]N. Vinothini
[2]G. Ananthi
[3]A.Subramaniya Siva
[4] N. Bhuvaneswari

Hybrid Energy Harvesting Framework for NBIoT Sensors: A Stochastic Geometry Approach

Journal of Electrical Systems

Abstract: - This paper presents a sustainable energy harvesting analysis for Narrowband Internet of Things (NB-IoT) sensors by integrating hybrid sources: Radio Frequency (RF) signals and carbon dioxide (CO_2) emissions from diesel-powered RF base stations. This research employs a spatial framework leveraging stochastic geometry to model the Probability Density Function (PDF) of distances, reflecting the spatial distribution of NB-IoT sensors and the variability of energy sources. Incorporating a Matern cluster process adds realism by capturing the clustering effects, crucial for understanding energy harvesting performance. The analysis focuses on optimizing the harvested energy while minimizing environmental impact, quantified by CO_2 emissions. A closed-form solution is derived to achieve this balance, offering practical insights into sustainable energy harvesting for low-power NB-IoT devices, promoting efficient energy usage, and reduced environmental footprint.

Keywords: RF energy, CO2 emission, Energy Harvesting, NBIoT sensors, Stochastic Geometry

I. INTRODUCTION

Energy harvesting has become increasingly vital in pursuing sustainable energy solutions. As we navigate the challenges posed by climate change, there is a growing emphasis on renewable energy sources for energy harvesting. However, despite this focus, there remains significant potential for innovation in other areas, particularly in Radio Frequency (RF) energy harvesting. Ambient RF Energy Harvesting is a cutting-edge technology that capitalizes on the omnipresent radio frequency signals in the environment to generate electrical power [1]. This technology presents a promising alternative in scenarios where conventional power sources, such as batteries, may be impractical or inconvenient to replace [2]. Moreover, with carbon footprints becoming unavoidable due to widespread industrial activities, utilizing the waste CO2 emitted into the environment for energy generation represents a unique and environmentally conscious approach to energy harvesting [3],[4]. Harvesting energy from CO2 emissions not only helps generate electricity but also serves as an effective strategy for carbon footprint reduction. This dual benefit of energy generation and environmental remediation adds a valuable dimension to the energy harvesting landscape. Research by [4] explores large-scale cooperative wireless networks using a stochastic geometry framework that integrates energy harvesting.

Recent advancements in flexible and stretchable energy harvesting devices underscore the transformative potential of these technologies. These devices can effectively power remote sensors, IoT devices, and other low-power electronics, reducing dependence on traditional energy sources [5]. This approach allows for realistic modeling of the spatial distribution of wireless devices and energy-harvesting elements [6]. The Voronoi Diagram serves as a foundational tool, creating non-overlapping polygons around each sensor node and enhancing the accuracy of localization techniques through geometric relationships [7]. Furthermore, [8] investigates the relationship between distance distributions and Matern cluster processes, emphasizing their relevance in analyzing network performance. The Matern cluster process effectively characterizes spatial patterns and clustering behaviours within a network,

[1] *QIP Research Scholar, Department of ECE, Thiagarajar college of Engineering, Madurai, India

[2] Associate Professor, Department of ECE, Thiagarajar college of Engineering, Madurai, India

[3] Assistant Professor, K. Ramakrishnan College of Engineering, Trichy, India

[4] Assistant Professor, SSM Institute of Engineering and Technology, Dindigul, India

[1] vinothinin@student.tce.edu, [2] gananthi@tce.edu, [3]npksiva.ss@gmail.com , [4] bhuvianuyogesh@gmail.com

providing insights into the distribution of distances among nodes [9],[10]. The study of these distance distributions is critical for optimizing energy harvesting strategies.

Estimating the carbon footprint from diesel generator emissions is crucial for understanding and mitigating the environmental impact of power generation [11]. This analysis involves meticulous calculations of greenhouse gas emissions, particularly carbon dioxide, produced during diesel generator operation [12],[13]. Harvesting energy from CO2 emissions represents an innovative and environmentally conscious approach to both energy generation and carbon footprint reduction [14],[15]. The process typically involves capturing and utilizing carbon dioxide emissions from industrial facilities or power plants. One method includes deploying advanced technologies like carbon capture and storage (CCS) [16],[17]. Another approach involves biological processes, such as algae cultivation, where microorganisms utilize CO2 to generate biomass or biofuels or convert it into graphene [18],[19].

The integration of energy-efficient Narrowband Internet of Things (NBIoT) applications also presents a significant opportunity for enhancing smart cities. Li, X., Wang, et al. provide a comprehensive examination of NBIoT's architecture and its applications, which range from smart cities to industrial automation [20],[21]. For instance, NBIoT-enabled sensors in parking lots can relay real-time information about parking space availability, optimizing traffic flow and reducing congestion [22],[23]. The design of smart home systems based on NBIoT further heralds a new era of intelligent living spaces [24],[25].

This paper's main contribution lies in employing a stochastic geometry approach using the Matern cluster process to analyze energy harvesting from CO2 emissions and RF signals at base stations. This innovative framework allows for robust and realistic modelling of spatial relationships among wireless devices and energy sources, which is crucial for understanding how energy harvesting systems perform in various deployment scenarios. By developing an energy harvesting framework that considers the locations of base stations and the distances between sources and NBIoT sensor nodes, the research aims to maximize energy efficiency. This consideration is vital in practical applications, where the spatial distribution of devices can significantly influence energy collection performance.

Moreover, the focus on both CO2 emissions and RF signals presents a holistic approach to energy harvesting, exploring synergies that can lead to more sustainable energy solutions. By incorporating distance probability density function (PDF) generation, the research enables a quantitative analysis of how distance impacts energy harvesting efficiency, contributing to the development of more effective energy harvesting strategies. This paper is structured into sections detailing the proposed system model and the energy harvesting framework in Sections 2 and 3, respectively. Simulated results supporting the proposed model are presented in Section 4, followed by conclusion.

II. SYSTEM MODEL

Consider the energy harvesting system for NBIoT sensors as the proposed system model shown in Fig 1. The energy harvester harvests the energy from dual sources like ambient Radio frequency energy from the base stations and CO2 emission from the diesel generators [10] in the RF base stations respectively.

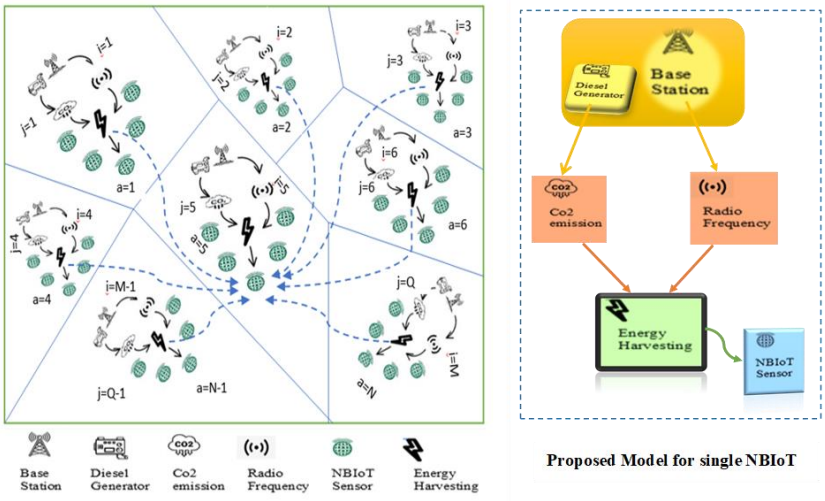

Fig 1. Proposed System Model

The received signal at NBIoT sensor can be represented as (1).

$$\sum_{a=1}^{N}\sum_{i=1}^{M}\sum_{j=1}^{Q} y_{NBIoT_{a,i,j}} = \sum_{a=1}^{N}\sum_{i=1}^{M} x_{RF_{a,i}} H_{P-RF}^{a,i} + \sum_{a=1}^{N}\sum_{j=1}^{Q} x_{C_{a,j}} H_{P-C}^{a,j} \quad (1)$$

We consider N number of sensor nodes for harvesting RF energy and CO2 emission-based energy from M number of ambient RF sources and Q number of CO2 emitting diesel generator sources from the RF base stations respectively. (1) describes the received signal ($y_{NBIoT_{a,i,j}}$) from the radio frequency signal ($x_{RF_{a,i}}$) in a free-space channel ($H_{\mathrm{P-RF}}^{a,i}$) in base stations and CO2 emissions from diesel generators in base stations ($x_{C_{a,j}}$) in a free-space channel which is $H_{\mathrm{P-C}}^{a,j}$. The noise is not included in our consideration. The harvested energy from the energy harvester is utilized for *N* number of NBIoT sensor nodes. The energy harvester is designed so that each sensor node has its harvesting elements separately depending on the nature of the source. From the proposed system model diagram, the first NBIoT sensor node is represented as a=1 for which the RF energy source is represented as i=1 and the diesel generator source for CO2 emission is represented as j=1. The stochastic model represented here is modeled for a=1,2,3……. N NBIoT sensor nodes with i=1,2,3…….M Radio Frequency sources and j=1,2,3…...Q number of diesel generator sources.

III. ENERGY HARVESTING FRAMEWORK

The RF energy harvesting rate by NBIoT sensor node a from RF energy source i in a free-space channel is $E_{\mathrm{P-RF}}^{a,i}$ and the CO2 emission-based energy harvesting rate by the NBIoT sensor node a from the CO2 emissions in diesel generator of base station j in a free space channel $E_{\mathrm{P-C}}^{a,j}$ can be obtained based on Friis equation [3] as

$$E_{P-RF}^{a,i} = \alpha_a RF_S^i \frac{G_{RF}^i G_X^a (\lambda_i)^2}{(4\pi dt_{a,i})^2} \quad (2)$$

$$E_{P-C}^{a,j} = \beta_b C_S^j \frac{G_C^j G_X^a (\lambda_j)^2}{(4\pi dt_{a,j})^2} \quad (3)$$

Where α_a is the Radio frequency power into DC power conversion efficiency of sensor node a. R_{FS}^i is the i^{th} energy source's RF transmitting power, G_{RF}^i transmitting antenna gain of i^{th} RF energy source, G_X^a is the gain of receiver antenna of sensor node, λ_i is wavelength of the RF energy source i. And similarly, β_b is CO2-to-power conversion efficiency of the sensor node a, C_S^j is the CO2 emissions transmitting power of energy source j , G_C^j is the gain of transmitting antenna of CO2 emissions energy source j , λ_j is the wavelength emitted at CO2 emissions energy source j . Let $x_a \in \mathbb{R}^2$, $x_i \in \mathbb{R}^2$ and $x_j \in \mathbb{R}^2$ represents the sensor node coordinates with RF energy source i, and CO2 emissions source j respectively.

$$dt_{a,i} = c + \|x_a - x_i\| \quad (4)$$

$$dt_{a,j} = c + \|x_a - x_j\| \quad (5)$$

Where $dt_{a,i}$, $dt_{a,j}$ be the distance between the transmit antenna of RF energy source i and the receiver antenna of sensor node a and distance between the CO2 emissions energy source j and the receiver antenna of sensor node a can be obtained from (4) and (5). And c is a finite and fixed parameter.

A. Theorem 1

The aggregated energy harvesting rate by NBIoT sensor node a can be obtained from (2) and (3) as in (6).

$$E_P = E_{\mathrm{P-RF}}^{a,i} + E_{\mathrm{P-C}}^{a,j} \quad (6)$$

To solve for the NBIoT sensor node's power utilization, the expected energy harvesting rate can be derived by the theorem 1 in [6].

$$E_P = \sum_{j\in\delta} \alpha_a RF_{\mathrm{S}}^i \frac{G_{RF}^i G_X^a (\lambda_i)^2}{(4\pi(c+\|x_a - x_i\|))^2} + \sum_{c\in\delta} \beta_b C_S^j \frac{G_C^j G_X^a (\lambda_j)^2}{\left(4\pi\left(c+\|x_a - x_j\|\right)\right)^2}$$

(7)

where δ is a random set consisting of all energy sources. Assume that δ is a point process.

$$\mathbb{E}[E_P] = \mathbb{Z}\int_R \frac{\rho^{(1)}(x)}{(c+\|x\|)^2}\mathrm{d}x + \int_R \frac{\rho^{(1)}(x)}{(c+\|x\|)^2}\mathrm{d}x \tag{8}$$

where, $\mathbb{Z} = [(\alpha_a + \beta_b)(R_S^i + C_S^j)(G_R^i + G_C^j)((\lambda_i)^2 + (\lambda_j)^2)\frac{G_X^a}{(4\pi)^2}]$

by Campbell's formula [27],

$$\mathbb{E}[E_P] = 2\pi\mathbb{Z}\int_0^R \frac{\rho.r}{(c+r)^2}\mathrm{dr} + 2\pi\int_0^R \rho\frac{\rho.r}{(c+r)^2}\mathrm{dr} \tag{9}$$

And the integral on the right-hand side of (9) is computed explicitly by polar change of variable as,

$$\int_0^R \frac{r}{(c+r)^2}\mathrm{d}r = \left(\frac{c}{R+c} + \ln(R+c) - 1 - \ln(c)\right) \tag{10}$$

Therefore, the expected energy harvesting rate of NBIoT sensor node a is as follows

$$\mathbb{E}[E_P] = \tau\left(\frac{c}{R+c} + \ln(R+c) - 1 - \ln(c)\right) \tag{11}$$

Where $\tau = \frac{\rho G_1 G_X^a \gamma T_P (\lambda_t)^2}{4\pi}$; $\gamma = (\alpha_a + \beta_b)$; $T_P = RF_S^i + C_S^j$; $\lambda_t = ((\lambda_i)^2 + (\lambda_j)^2)$; $G_1 = (G_{RF}^i + G_C^j)$

The distribution of the distance between sensor nodes and harvesting energy sources is considered as the Matern cluster process. The Matern cluster process could refer to a spatial point process where the spatial distribution of points follows a Matern-type model. This might involve clusters of points characterized by the Matern covariance function, which is often used in spatial statistics. The radii of all clusters are R. A point outside any cluster is referred to as the exterior point for that cluster. Meanwhile, interior points are evenly distributed within each cluster, following a Poisson distribution with an average count of $\bar{n}$. This distribution is effectively captured by the conditional probability density function of an interior point v within a cluster centered at x_0 is in (12)

$$f_{R_d}(v \mid x_0) = \frac{1}{\pi R^2}\ for\ r = \|v - \boldsymbol{x}_0\| \le R \tag{12}$$

Where $0 \le d \le 2R$. Analysing the distance distribution between interior and exterior points within the same cluster is essential for gaining insights into the spatial dynamics and clustering behaviour inherent in the Matern cluster process. By providing the distance PDF, the complexity of analyzing these metrics will be decreased [14].

B. Theorem 2

Let R_d be a random variable that denotes the distance between an interior point and an exterior point of a Matern cluster with radius *R* [15].

The probability density function (PDF) for the distance D between two interior points belonging to a Matern cluster can be expressed as (13).

$$f_{\mathrm{D}}(\mathrm{d}) = \frac{4d}{\pi R^2}\left(arccos\left(\frac{d}{2R}\right) - \left(\frac{d}{2R}\right)\sqrt{1 - \left(\frac{d}{2R}\right)^2}\right) \tag{13}$$

The probability density function (PDF) for the distance *D* between an interior point and an exterior point within a Matern cluster can be expressed in (14)

$$f_{R_c}(r_c \mid R_n) = \frac{c(r_c)}{\pi R^2} \qquad \text{where for } R_n > R \tag{14}$$

$$c(r_c) = \begin{cases} c_1(r_c), & r_c \in [R_n - R, R_n + R] \\ 0, & \text{otherwise} \end{cases} \tag{15}$$

$$c_1(r_c) = 2r_c arcsin\left(\sqrt{\frac{4R_n^2 r_c^2 - (R_n^2 - R^2 + r_c^2)}{2R_n r_c}}\right) \qquad \text{Otherwise,}$$

$$c(r_c) = \begin{pmatrix} 2\pi r_c\,, & r_c \le R - R_n \\ 2\pi r_c - c_1(r_c)\,, & R - R_n \le r_c \le \sqrt{R^2 - R_n^2} \\ c_1(r_c)\,, & \sqrt{R^2 - R_n^2} < r_c \le R + R_n \\ 0\,, & Otherwise \end{pmatrix} \tag{16}$$

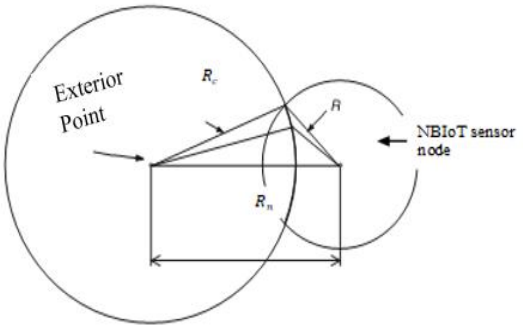

Fig.2. The Exterior point lies outside the cluster

When R_n exceeds R, the potential positions for the interior point, equidistant to the exterior point, lies along the circular arc within the confines of the cluster, as illustrated in Figure 2. As R_C progresses from $R_n - R$ to $R_n + R$, the cluster can accommodate numerous non-overlapping arcs, each delineating a set of points with identical distances from the exterior point. Consequently, by determining the arc length using equation (15), the associated density for R_C is attained in equation (14).

When $0 < R_n \leq R$,the exterior point is situated within the Matern cluster. The potential locations of the interior point, equidistant from an exterior point, can occur in two scenarios: (i) on the circle centered at an exterior point $R_c \leq R - R_n$, as depicted in Figure 3; (ii) on the circular arc of a circle with radius R_c enclosed by the cluster with a radius of R, as illustrated in Figures 3 and 4. The first scenario corresponds to the perimeter of a circle with a radius R_c, representing the initial case in (16). The latter scenario encompasses the second and third cases in (16), which $\sqrt{R^2 - R_n^2}$ serves as the boundary to determine whether the circular arc enclosed by the cluster is the major or minor arc of a circle with a radius R_c.

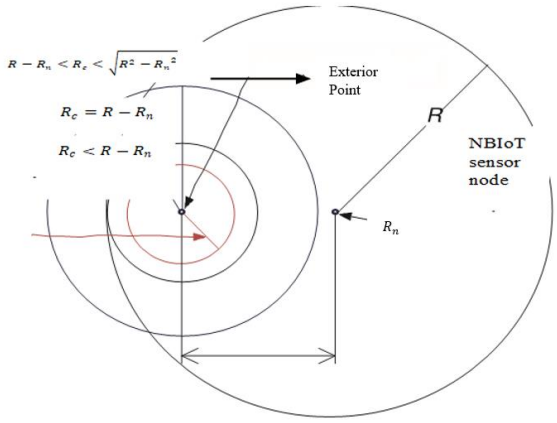

Fig. 3. The Exterior point resides within the cluster.

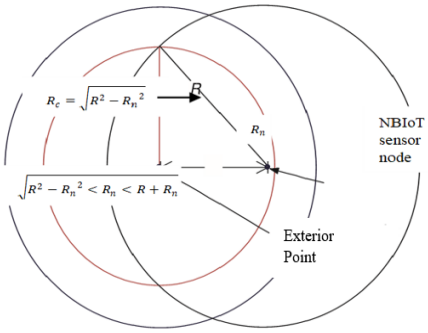

Fig. 4. The Exterior point is situated within the cluster

In the special case where $R_n = 0$, the exterior point coincides with the cluster origin. The potential locations of the interior point, equidistant from the exterior point, form a circle with radius R_c centered at the cluster origin. This scenario aligns with the first case outlined in (16). Thus, this completes our proof. The distance PDF function of the expected energy harvesting rate of the NBIoT Sensor can be derived from Eqn (14).

$$f_{\mathrm{R}}(\mathrm{R}) = 2r_c \int_0^R \frac{c+\ln\,(R+c)^2}{R^2(R+c)}\,dR \tag{17}$$

From Table of Integrals [26],

$$ln\frac{x^2}{x^3}dx = -\frac{\log(x^2+1)}{2x^2} + \Psi \tag{18}$$

From Eqn (19), the corresponding density r_c can be achieved in (19)

$$f_{\mathrm{R}}(\mathrm{R}) = -\frac{r_c log(R)^2+1}{R^2}\Psi \tag{19}$$

The energy harvesting rate of NBIoT sensor node a is derived for (11) in (20)

$$E_{P-NBIoT} = \tau\left(\frac{r_c log(R)^2+1}{R^2} + \Psi\right) \tag{20}$$

Where Ψ is constant. The energy harvesting rate for NBIoT sensor node $(E_{P-NBIoT})$ in (20) depends on the parameter τ which has the intensity function ρ, total transmitting gain of two RF sources G_1, gain of the receiver antenna of the sensor node G_X^a, total power conversion efficiency factor γ, total transmitting power T_P and, total wavelength λ_t.

IV. Results and Discussion

The parameters used for energy harvesting analysis for NBIoT sensor nodes are described in Table 1 and 2.

Table1. The carbon footprints (kgCO2/Day) and (kgCO2/kWh) corresponding to different rated power levels of a diesel generator are examined alongside their respective emission factors(kgCo2/litre)

Sl. No	**Rated Power of Diesel Generator in kW**	**Emission Factor (kgCo2/litre)**									
1	2	2.56	5.11	7.67	10.22	12.78	0.41	0.81	1.22	1.63	2.03
2	3	3.06	6.12	9.18	12.24	15.30	0.49	0.97	1.46	1.95	2.44
3	4	3.57	7.13	10.70	14.26	17.83	0.57	1.13	1.70	2.27	2.84
4	5	4.07	8.14	12.21	16.28	20.35	0.65	1.30	1.94	2.59	3.24

Table 2. Simulation Parameters

Sl. No	Parameter	Specification
1	Core Radius	0.1
2	Number of Base stations	10
3	Density of sensor nodes	10,20,30 numbers
4	Wavelength	110.6×10^{-6}
5	Transmitting antenna gain	1dB
6	Receiver antenna gain	1dB
7	Energy conversion efficiency	1
8	Distance	10m to 100m

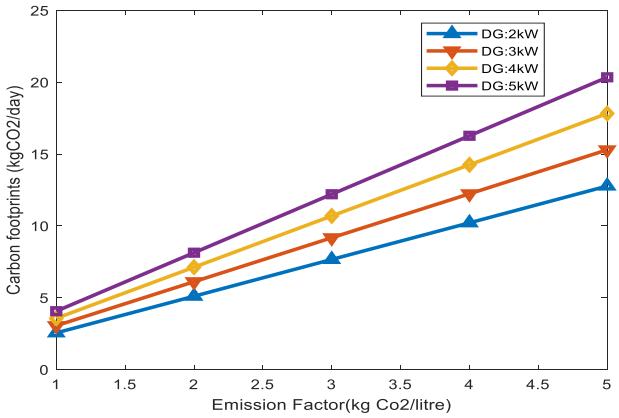

Fig. 5. Emission factor(kgCo2/liter) vs Carbon footprints(kgCo2/day)

Figure 5 Analyses the relationship between carbon footprints measured in KgCO2/day, and emission factors, measured in KgCO2/liter. It shows the efficiency of resource use, with a steeper slope suggesting higher carbon emissions associated with each unit of resource consumption. Higher emission factors (KgCO2/litre) mean that the production or consumption of a particular resource (Diesel generator with 5kW capacity) results in more carbon emissions.

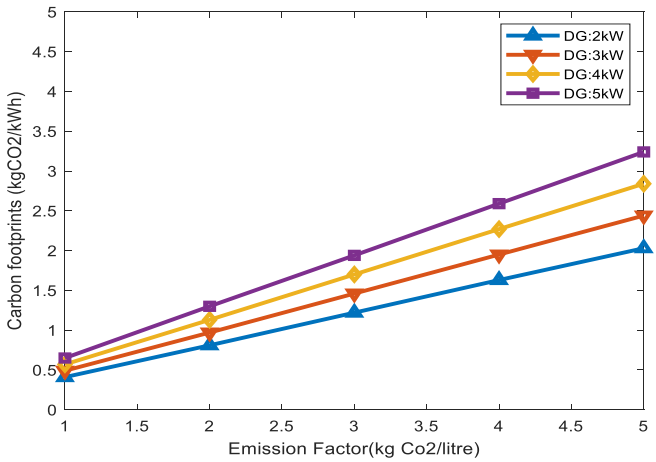

Fig. 6. Emission factor(kgCo2/Litre) vs Carbon footprints(kgCo2/kWh)

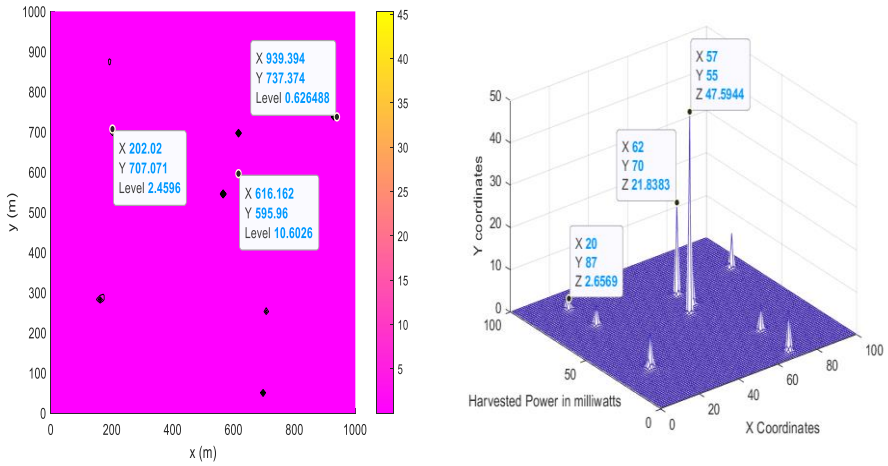

Fig. 7. Base station location coordinates vs. harvested Power(W)

Figure 6 can provide insights into the carbon efficiency of different energy sources. A lower emission factor indicates cleaner, more sustainable energy production. A rising trend in the plot could indicate that larger diesel generators tend to have higher emission factors, resulting in increased carbon footprints per unit of electricity generated. Therefore, a negative correlation or a downward trend in the plot suggests that, on average, carbon footprints decrease as the emission factor decreases, reflecting a shift towards cleaner energy sources. In Figure 7, For various location points of base stations, the harvested power is analyzed. if the X, and Y coordinates of base stations increase then the harvested energy decreases. For the location at (616m,595m) the energy harvested is a maximum of 10.6w in the left side figure. In the figure on the right, an increase in both X and Y coordinates corresponds to a decrease in harvested power, transitioning from 47.5W and 21.83W to 2.65W

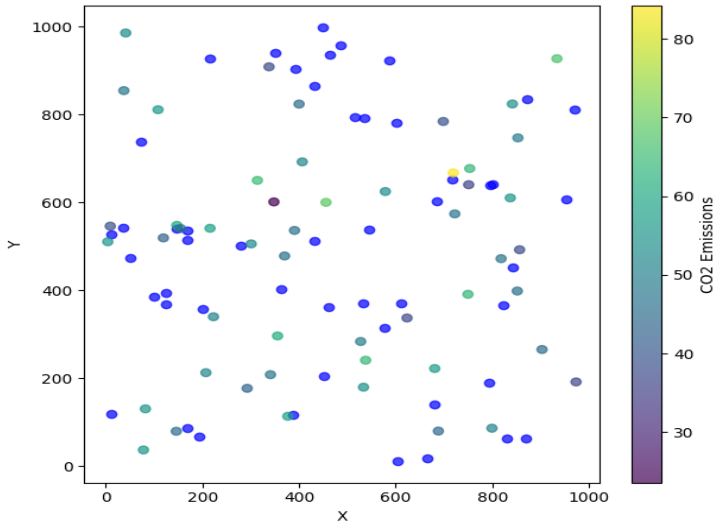

Fig. 8. NBIoT Sensor Nodes deployment with RF and CO2 Energy Sources

Figure 8 illustrates a stochastic analysis of NB-IoT sensor nodes' localization from two distinct sources: RF signals and CO2 emissions from a base station. In the figure blue circle depicting RF localization, the spatial distribution of sensor nodes reveals noticeable clustering patterns, suggesting regions with a higher concentration of these nodes. The colormap represents CO2 emissions localization in which the color intensity reflects varying levels of emissions, providing insights into the spatial distribution of environmental impact. Fig. 9 shows that the distance between the source and the energy harvester has a prominent impact on the harvested power. If the distance is increased from 10m to 100m, it gives the highest harvested power at a 10m distance. When the number of sensor nodes increases from 10 to 30 numbers with the distance, the harvested power will be raised to 6.5nw from 2.1nw. As the number of NB-IoT sensor nodes rises, the inference drawn from the plot becomes multifaceted. The plot

allows for the identification of optimal distances for power generation while considering the cumulative impact of multiple sensor nodes on the available energy.

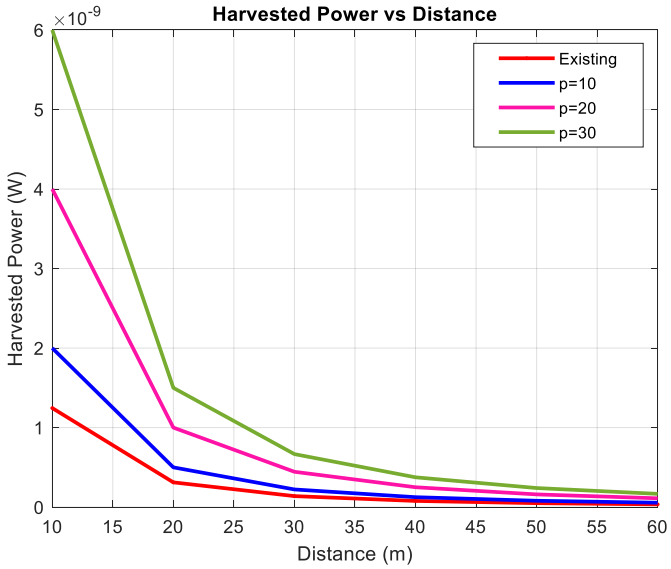

Fig 9. Distance(m) vs Harvested Power(W)

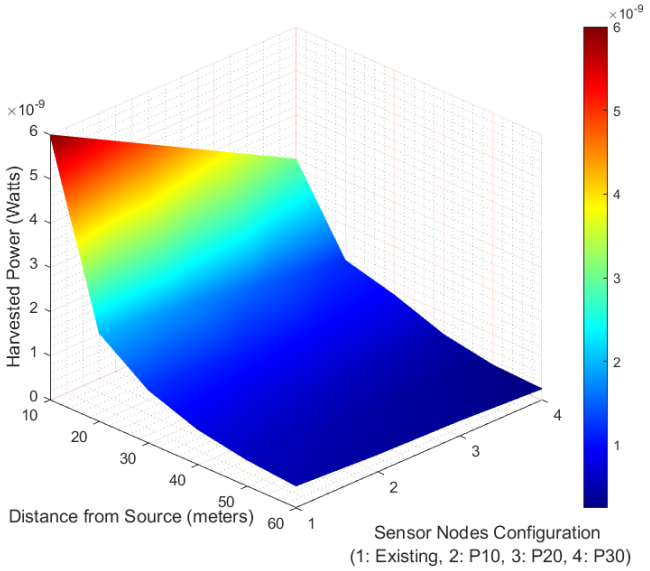

Fig 10. 3D Surface Plot: Harvested Power at Specific Distances for Different Configurations

The 3D plot in Fig. 10 shows that as the distance from the energy source increases, the harvested power from RF and CO_2 emissions decreases significantly. This drop in power becomes more noticeable at distances beyond 40 meters. However, higher configurations (P10, P20, P30) result in more harvested power compared to the existing setup, indicating that increasing the number of sensor nodes or enhancing the setup boosts energy collection. Overall, the plot highlights how distance and configuration choices greatly impact the effectiveness of energy harvesting.

V. CONCLUSION

In this paper, we proposed the energy harvesting analysis for NBIoT sensor nodes from RF energy and CO2 emissions in base stations. The analysis shows that the maximum harvested energy is achieved with a minimum distance between the base stations and sensor nodes. If the distance is increased from 10m to 100m, it provides maximum harvested power at a 10m distance. When the number of sensor nodes increases from 10 to 30 with the distance, the harvested power will be raised to 6.5nW from 2.1nW. The harvested energy can be used to power low-

power electronic devices and NB-IoT sensors which are designed to enable efficient communication between devices in the Internet of Things (IoT). NB-IoT technology can help utilities optimize their operations, reduce costs, and improve the reliability and sustainability of the Smart grid. Also, the harvested energy from CO2 emissions has a potential solution for large-scale energy storage as it could provide a way to capture and store carbon emissions from base stations, and other industrial sources.

ACKNOWLEDGMENT

This work was supported under the Quality Improvement Programme - AICTE -Full-Time Ph.D. Programme in the Department of Electronics and Communication Engineering at Thiagarajar College of Engineering, Madurai (Tamil Nadu).

REFERENCES

[1] Akinaga, H. (2020). Recent Advances and future prospects in Energy Harvesting Technologies, Japanese Journal of Applied Physics, 59(11), 110201

[2] W. M. D. R. Gunathilaka, H. G. C. P. Dinesh, G. G. C. M. Gunasekara, K. M. M. W. N. B. Narampanawe and J. V. Wijayakulasooriya, "Ambient Radio Frequency energy harvesting," 2012 IEEE 7th International Conference on Industrial and Information Systems (ICIIS), Chennai, India, 2012, pp. 1-5, doi: 10.1109/ICIInfS.2012.6304789.

[3] H. J. Visser and R. J. M. Vullers, "RF Energy Harvesting and Transport for Wireless Sensor Network Applications: Principles and Requirements," in Proceedings of the IEEE, vol. 101, no. 6, pp. 1410-1423, June 2013, doi: 10.1109/JPROC.2013.2250891.

[4] Talha, K., Orlik, P., Kim, K. K., Heath, R. W., & Sawa, K. (2017). A Stochastic Geometry Analysis of Large-Scale Cooperative Wireless Networks Powered by Energy Harvesting. IEEE Transactions on Communications.

[5] Liu, Q., & Ball, E. (2020). A tractable stochastic geometry model of coverage and an approach to energy efficiency estimation in LPWAN networks. International Journal of Sensor Networks, 33(4), 211. https://doi.org/10.1504/ijsnet.2020.10031340

[6] Flint, I., Lu, X., Privault, N., Niyato, D., & Wang, P. (2014a). Performance analysis of ambient RF energy harvesting: A stochastic geometry approach. ArXiv (Cornell University).

[7] C. He, S. Guo and Y. Yang, "Voronoi diagram based indoor localization in wireless sensor networks," 2015 IEEE International Conference on Communications (ICC), London, UK, 2015, pp. 3269-3274, doi: 10.1109/ICC.2015.7248828.

[8] Tang, Jinchuan, et al. "Distance distributions for Matérn cluster processes with application to network performance analysis." 2017 IEEE International Conference on Communications (ICC). IEEE, 2017

[9] F. Voss, C. Gloaguen, F. Fleischer and V. Schmidt, "Distributional properties of Euclidean distances in wireless networks involving road systems," in IEEE Journal on Selected Areas in Communications, vol. 27, no. 7, pp. 1047-1055, September 2009, doi: 10.1109/JSAC.2009.090903.

[10] A. Q. Jakhrani, A. R. H. Rigit, A. -K. Othman, S. R. Samo and S. A. Kamboh, "Estimation of carbon footprints from diesel generator emissions," 2012 International Conference on Green and Ubiquitous Technology, Bandung, Indonesia, 2012, pp. 78-81, doi: 10.1109/GUT.2012.6344193.

[11] Talieh Rajabloo ,Joris Valee , Yves Marennee, Leo Coppensf, Ward De Ceuninck ," Carbon capture and utilization for industrial applications", 2022 International Joint Conference on Energy and Environmental Engineering (CoEEE 2022), Stockholm, Sweden(virtually), June 24–26, 2022 Energy Reports, Volume 9, Supplement 2, April 2023, Pages 111-116

[12] De Morais, A. M., Justino, M. a. M., Valente, O. S., De Morais Hanriot, S., & Sodré, J. R. (2013). Hydrogen impacts on performance and CO2 emissions from a diesel power generator. International Journal of Hydrogen Energy, 38(16), 6857–6864. https://doi.org/10.1016/j.ijhydene.2013.03.119

[13] Hamelers, Hubertus V. M. et al. "Harvesting Energy from CO2 Emissions." Environmental Science and Technology Letters 1 (2014): 31-35.

[14] Krishnan, S.S., Balasubramanian, N., & Ramakrishnan, A.M. (2012). Energy consumption and CO2 emissions by the Indian mobile telecom industry. Int. J. Crit. Infrastructures, 8, 156-168.

[15] Alaba, P.A., Mazari, S.A., Farouk, H.U. et al. Harvesting Electricity from CO2 Emission: Opportunities, Challenges and Future Prospects. Int. J. of Precis. Eng. and Manuf.-Green Tech. 8, 1061–1081 (2021).

[16] Lamiaa Abdallah, Tarek El-Shennawy, "Reducing Carbon Dioxide Emissions from Electricity Sector Using Smart Electric Grid Applications", Journal of Engineering, vol. 2013, Article ID 845051, 8 pages, 2013.

[17] Molina-Jirón, Concepción et al. "Direct Conversion of CO2 to Multi-Layer Graphene using Cu–Pd Alloys." Chemsuschem 12 (2019): 3509 - 3514.

[18] J.M. Paz-Garcia, J.E. Dykstra, P.M. Biesheuvel, H.V.M. Hamelers, Energy from CO2 using capacitive electrodes – A model for energy extraction cycles, Journal of Colloid and Interface Science, Volume 442, 2015, Pages 103-109, ISSN 0021-9797, https://doi.org/10.1016/j.jcis.2014.11.045.

[19] Boot-Handford, M. E., Abanades, J., Anthony, E. J., Blunt, M. J., Brandani, S., Mac Dowell, N., Fernández, J. R., Ferrari, M., Groß, R., Hallett, J. P., Haszeldine, R. S., Heptonstall, P., Lyngfelt, A., Makuch, Z., Mangano, E., Porter, R., Pourkashanian, M., Rochelle, G. T., Shah, N., . . . Fennell, P. S. (2014). Carbon capture and storage update. Energy and Environmental Science, 7(1), 130–189. https://doi.org/10.1039/c3ee42350f

[20] Li, X., Wang, X., Hu, X., Xu, C., Shao, W., & Wu, K. (2023). Direct conversion of CO2 to graphene via vapor–liquid reaction for magnesium matrix composites with structural and functional properties. Journal of Magnesium and Alloys, 11(4), 1206–1212. https://doi.org/10.1016/j.jma.2021.06.012

[21] Mikulčić, H., Skov, I. R., Dominković, D. F., Alwi, S. R. W., Manan, Z. A., Tan, R. G. R., Duić, N., Mohamad, S. N. H., & Wang, X. (2019). Flexible Carbon Capture and Utilization technologies in future energy systems and the utilization pathways of captured CO2. Renewable & Sustainable Energy Reviews, 114, 109338. https://doi.org/10.1016/j.rser.2019.109338

[22] Ravi, M., Rathore, S. K., & Murugan, S. (2023). Experimental investigations of CO2 capture using adsorbents in a standby power generation unit. Research Square (Research Square). https://doi.org/10.21203/rs.3.rs-2446846/v1

[23] Routray, S. K., Gopal, D., Pallekonda, A. K., Javali, A., & Kokkirigadda, S. (2021). Measurement, Control and Monitoring in Smart Grids using NBIoT. V. https://doi.org/10.1109/icict50816.2021.9358604

[24] Popli, S., Jha, R. K., & Jain, S. (2019). A survey on Energy Efficient Narrowband Internet of Things (NBIOT): architecture, application and challenges. IEEE Access, 7, 16739–16776. https://doi.org/10.1109/access.2018.2881533

[25] Han, C., Zhang, W., Li, M., & Tian, Y. (2022). Design of smart home system based on NB-IOT. Journal of Physics, 2254(1), 012039. https://doi.org/10.1088/1742-6596/2254/1/012039

[26] Van Haeringen, H., & Kok, L. (1982). Table errata: Table of integrals, series, and products [corrected and enlarged edition, Academic Press, New York, 1980; MR 81g:33001] by I. S. Gradshteyn [I. S. Gradshteĭn] and I. M. Ryzhik. Mathematics of Computation, 39(160), 747–757

[27] O. Kallenberg, Random measures, fourth ed. Berlin, Germany: Akademie-Verlag, 1986.